

RESEARCH

Open Access



NnARF17 and *NnARF18* from lotus promote root formation and modulate stress tolerance in transgenic *Arabidopsis thaliana*

Cheng Libao^{1*}, Liang Shiting¹, Zhao Chen¹ and Li Shuyan^{2*}

Abstract

Auxin response factors (ARFs) play a crucial role in regulating gene expression within the auxin signal transduction pathway, particularly during adventitious root (AR) formation. In this investigation, we identified full-length sequences for *ARF17* and *ARF18*, encompassing 1,800 and 2,055 bp, encoding 599 and 684 amino acid residues, respectively. Despite exhibiting low sequence homology, the *ARF17*- and *ARF18*-encoded proteins displayed significant structural similarity and shared identical motifs. Phylogenetic analysis revealed close relationships between *NnARF17* and *VvARF17*, as well as *NnARF18* and *BvARF18*. Both *ARF17* and *ARF18* demonstrated responsiveness to exogenous indole-3-acetic acid (IAA), ethephon, and sucrose, exhibiting organ-specific expression patterns. Beyond their role in promoting root development, these ARFs enhanced stem growth and conferred drought tolerance while mitigating waterlogging stress in transgenic *Arabidopsis* plants. RNA sequencing data indicated upregulation of 51 and 75 genes in *ARF17* and *ARF18* transgenic plants, respectively, including five and three genes associated with hormone metabolism and responses. Further analysis of transgenic plants revealed a significant decrease in IAA content, accompanied by a marked increase in abscisic acid content under normal growth conditions. Additionally, lotus seedlings treated with IAA exhibited elevated levels of polyphenol oxidase, IAA oxidase, and peroxidase. The consistent modulation of IAA content in both lotus and transgenic plants highlights the pivotal role of IAA in AR formation in lotus seedlings.

Key message

Indole-3-acetic acid significantly influences the formation of short-borne roots in lotus seedlings. The overexpression of two auxin-responsive genes, *NnARF17* and *NnARF18*, in *Arabidopsis* resulted in enhanced root development.

Keywords lotus, Adventitious root, *NnARF17*, *NnARF18*, *Arabidopsis*

*Correspondence:

Cheng Libao
lbcheng@yzu.edu.cn
Li Shuyan
lsydbnd@163.com

¹College of Horticulture and Landscape Architecture, Yangzhou University, Yangzhou, Jiangsu, P. R. China

²College of Guangling, Yangzhou University, Yangzhou, Jiangsu, P. R. China



© The Author(s) 2024. **Open Access** This article is licensed under a Creative Commons Attribution 4.0 International License, which permits use, sharing, adaptation, distribution and reproduction in any medium or format, as long as you give appropriate credit to the original author(s) and the source, provide a link to the Creative Commons licence, and indicate if changes were made. The images or other third party material in this article are included in the article's Creative Commons licence, unless indicated otherwise in a credit line to the material. If material is not included in the article's Creative Commons licence and your intended use is not permitted by statutory regulation or exceeds the permitted use, you will need to obtain permission directly from the copyright holder. To view a copy of this licence, visit <http://creativecommons.org/licenses/by/4.0/>. The Creative Commons Public Domain Dedication waiver (<http://creativecommons.org/publicdomain/zero/1.0/>) applies to the data made available in this article, unless otherwise stated in a credit line to the data.

Introduction

Lotus root (*Nelumbo nucifera* Gaertn) is a member of the Nymphaeaceae family, which encompasses only one other species: *Nelumbo lutea* [1, 2]. It serves as a significant off-season vegetable [3] and has one of the largest aquatic vegetable production areas in China, particularly in the southern regions of the Yangtze River Basin, including Hubei, Hunan, Jiangsu, Guangdong, Guangxi, and Jiangxi. These areas provide optimal climatic conditions for lotus root growth, generating substantial profits for local farmers. Beyond its role as a vegetable, lotus is utilized in various products, such as drinks, tea, salt lotus, and glutinous rice lotus, which have gained international popularity [4]. Due to its rich composition of special substances, lotus root is recognized as a functional food or medicine.

The short-borne roots (adventitious roots (ARs)) of lotus play a crucial role in plant growth and the formation of storage organs, compensating for the underdevelopment of the primary root. Any factor promoting the development of ARs contributes to enhanced plant metabolism and increased yield of storage organs. Root systems in plants exhibit diverse morphologies influenced by genetic and environmental factors. Plant roots are categorized into tap roots (primary roots), basal roots, ARs, and lateral roots based on their occurrence [5]. Lotus plants, in particular, may exhibit severe degeneration of the main root, leading to the production of numerous ARs in the hypocotyl of seedlings or the internodes of storage organs to sustain normal growth. The ARs are considered secondary root systems, and their formation involves three biological stages: induction, initiation, and expression [6, 7]. The initial stage involves the transition of cell function, where normal cells differentiate into meristematic cells capable of developing into ARs. The second stage is the primordial establishment, during which meristematic cells differentiate into primordial ARs [8]. In the final stage, the AR primordium continues to develop, leading to the breakout of the stem or leaf epidermis, resulting in fully formed ARs [9]. This entire developmental process is tightly regulated by multiple factors, including genetic elements (gene regulators, and microRNAs) and environmental conditions [8]. Consequently, AR formation is considered a heritable quantitative trait [10].

Indole-3-acetic acid (IAA) stands as a pivotal plant hormone crucial for regulating various facets of plant growth and development. Serving as an essential regulator, it plays a fundamental role in cell division, elongation, and differentiation [11, 12]. Additionally, IAA collaborates with other factors to influence organ formation, playing a key role in processes such as primordial root induction, bud differentiation, leaf development, flowering, and fruit formation [13, 14]. In particular, auxin, a type of IAA,

triggers the development of the root cap, promotes root formation during the initiation stage, and facilitates the occurrence of ARs [15, 16], with a close correlation to auxin transport [17, 18]. Reports indicate that increased endogenous IAA levels or decreased IAA oxidase (IAAO) activity accelerate AR development [19, 20]. Exogenous IAA significantly influences AR formation by promoting cell division and primordium formation [11, 12]. Notably, the role of IAA in lotus AR formation is dose-dependent, with low concentrations dramatically accelerating AR development and high concentrations exhibiting the opposite effect [21]. The impact of abscisic acid (ABA) on AR formation is both dose- and species-specific. Generally, ABA signaling negatively affects AR development [22]. Further investigations reveal that ABA primarily inhibits AR formation during the induction stage of the primordium and the root elongation stage in softwood cuttings [23]. In the case of rice, ABA inhibits the rate of AR growth by influencing gibberellin A (GA) biosynthesis and IAA signaling [24]. The ABA / (IAA+GA3) ratio serves as an indicator of rooting capacity [25].

Auxin response factors (ARFs) play a crucial role in various plant physiological processes, encompassing the development of leaves, flowers, and roots, as well as processes like maturation, senescence, fruit abscission, and stress response. ARFs actively participate in the development of roots, including primary, lateral, and ARs, in plants. In *Arabidopsis*, *AtARF2* is recognized as a pivotal factor regulating root tip cell division, thereby influencing the formation of primary roots [26]. Additionally, *atARF10/atARF16* plays a role in root development by influencing root cap formation [27]. This phenomenon is also observed in rice, where the role of *OsARF1* is closely associated with root cap development [28]. In *OsARF12*-mutant rice, there is a decrease in root expansion, leading to a significant reduction in the number of primary roots [29]. Transgenic plants with constitutive expression of *atARF7* exhibit enhanced lateral root formation compared to wild-type plants [30]. Further analysis reveals that *AtARF7* interacts with MYB transcription factors to regulate lateral roots [31]. It is noteworthy that the roles of ARFs can vary among species. For instance, the overexpression of *ARF17* in *Arabidopsis* results in a significant decrease in the number of ARs [32], while *PeARF17* promotes the formation of ARs in transgenic plants [33].

Previously, our research revealed the significant influence of IAA on the formation of ARs in lotus seedlings [34]. Building on this, we identified *NnARF17* and *NnARF18* as key players in AR development. Given their association with the IAA signal transduction pathway, we hypothesized that *NnARF17* and *NnARF18* could serve as crucial regulators in the process of AR formation in lotus. This study aimed to provide a detailed analysis of the isolation of *NnARF17* and *NnARF18*, their expression

in lotus, and their primary functions in transgenic *Ara-bidopsis* plants. Additionally, we explored the potential pathways involved in root formation in these transgenic plants. The insights gained from this investigation contribute to a better understanding of the role of IAA signaling and establish a necessary foundation for further exploration of the regulatory networks governing AR formation in lotus seedlings.

Materials and methods

Preparation of plant materials

For our experiments, Taikong Lotus 36, a seed lotus variety widely cultivated in China, was chosen due to its abundant seed production. This lotus variety, developed by The Guangchang Bailian Institute, was procured from a market and sown in an experimental field of aquatic vegetables at Yangzhou University, Southeast China. Throughout the growth season (April to October), the field maintained a water depth of 20–25 cm from April to June, increased to approximately 40–50 cm in the summer months (July to August), and then returned to 20–30 cm in autumn (September to October). The average temperature was kept within the range of 25–35 °C during the day and 18–25 °C at night to support optimal plant growth. After harvesting, the seeds were stored at about 10–20 °C in a glass container.

The influence of exogenous IAA on ARs formation in lotus seedlings

To initiate the germination process, the lotus seed coat was ruptured, and the seeds were immersed in water at 26 °C in darkness for approximately 6 days. Fifty seedlings, each with two leaves, were selected and treated with 10 μM IAA for 2 days, after which they were transferred into water for continuous cultivation. The abundance of ARs was observed at 0, 2, 4, 6, and 8 days, with ARs measuring ≥ 0.2 cm in length from the epidermis being used for counting. Control plants, treated with water, were included in the experiment for comparison, and the entire process was conducted in triplicate.

Moreover, hypocotyls from both the treated and control plants were chosen for microstructural analysis at six different time points. The hypocotyls were sectioned into pieces measuring 3 × 3 × 2 mm (length × width × height) and then placed in a glass container filled with fixing fluid (free fatty acids, more than 20 times the volume of the samples). The container, containing the fixed sample, underwent a vacuum process using a syringe for approximately 5 s, followed by a 5 min opening. This cycle was repeated three times, and the containers were then transferred to room temperature for approximately 12–24 h. Subsequently, the samples underwent dehydration using ethanol at concentrations of 50%, 70%, 85%, 95%, and absolute for 30 min each. Following dehydration, a

mixture of absolute ethanol and pure xylene (1:1, v/v) was applied, followed by pure xylene for 30 min. Paraffin debris was used to fill the container containing the samples, and it was placed on a platform at room temperature for at least 12 h to prepare paraffin blocks. The paraffin blocks were sliced using a microtome to produce wax tape (10 microns in thickness), which was then transferred to a glass slide. The wax tape underwent sequential treatments of pure xylene, a mixed solution of xylene and absolute ethanol (1:1), and absolute ethanol, each for 5–10 min. Finally, the microstructure of the developed ARs was visualized using an optical microscope after the slide was air-dried.

Cloning of *NnARF17* and *NnARF18*

The expression levels of *NnARF17* and *NnARF18* during AR formation in lotus seedlings, as revealed by transcriptome data [35], prompted the cloning of these genes. The full-length sequences of *NnARF17* and *NnARF18* were sourced from the National Center for Biotechnology Information (NCBI) database. Gene-specific primers were designed using Primer 5.0 software. *NnARF17*: forward primer, 5'-ATGGCGTTGCAGAGGGTGAG T-3'; reverse primer, 5'-TAAGGAACAAGCTTCCACT GCTGAG-3'. *NnARF18*: forward primer, 5'-ATGGCGT ATGGAGATAGCTG-3'; reverse primer, 5'-TATCTCAG TCTTTAGGTCTGAATCC-3'. Total RNA was extracted from lotus leaves using the RNeasy MinElute Cleanup Kit (QIAGEN, Hilden, Germany), following the manufacturer's instructions. DNA contamination was eliminated through DNAase I treatment before synthesizing the first cDNA strand. The PCR system included 2.5 μL of dNTPs, 2 μL of each primer (forward and reverse), 2.5 μL of MgCl₂, 2 μL of Taq polymerase (5 U), 2 μL of cDNA fragments, and 7 μL of dH₂O in a total reaction volume of 20 μL. The PCR program consisted of pre-denaturation at 94 °C for 1 min; 35 cycles of denaturation at 94 °C for 1 min, annealing at 56–60 °C for 1 min, and extension at 72 °C for 1 min; and a final extension at 72 °C for 10 min. The target gene fragments were purified using the GeneJET Gel Extraction Kit (Thermo Fisher Scientific, Waltham, MA, USA) and inserted into a cloning vector (pMD 18-T vector; TaKaRa, Kusatsu, Japan). Recombination of these gene fragments was achieved using *DH5α*, and the resulting sequences were verified by Sangon Biotechnology Co., Ltd. (Shanghai, China).

Sequence analysis of *NnARF17* and *NnARF18*

For the comparative analysis of *NnARF17* and *NnARF18* sequences, DNAMAN (<https://www.onlinedown.net/article/10009213.htm>) was employed. To identify conserved domains, the Simple Modular Architecture Research Tool software program was utilized. The construction

of phylogenetic trees for *NnARF17* and *NnARF18* was accomplished using DNAMAN and MEGA X software.

Analysis of conserved motifs in *NnARF17* and *NnARF18* was performed using DNAMAN and the online software program MEME server v5.4.1 (<http://meme-suite.org/tools/meme>). The sequences of *NnARF17* and *NnARF18* were standardized and then submitted to the MEME software. In the system options, “zoops” and “ten” motifs in the required box were set according to the instructions. Finally, TBtools software was utilized to visualize the output.

Expression profiling analysis of *NnARF17* and *NnARF18*

The quantitative reverse transcription polymerase chain reaction (qRT-PCR) technique was employed to assess the expression levels of *NnARF17* and *NnARF18* in lotus seedlings subjected to treatments with 10 μ M IAA, 20 g/L sucrose, and 200 mg/L ethephon. Plant samples treated at five time-points (0, 2, 4, 6, and 8 days) were selected, and total plant RNA was extracted using the RNeasy MinElute Cleanup Kit (QIAGEN).

Gene expression was analyzed in various plant organs, including ARs, leaves, stems, flowers, and fruits. Genomic DNA contamination was removed using DNase I, and first-strand cDNA was synthesized with 3 μ g of purified RNA utilizing the RevertAid First Strand cDNA Synthesis Kit (Fermentas, Waltham, MA, USA). The following primers were used. *NnARF17*: forward primer: 5'-TCTGTGCAGAATCGTGTCGGTTATG-3', reverse primer: 5'-GAACTTACTCCACCCAGTCGTCAAC-3'; *NnARF18*: forward primer, 5'-ATGAGCCGACGAGTCCTGATCC-3', reverse primer, 5'-CCGTGGTTGACCTCTGAAGATGTG-3'. β -Actin served as the internal standard with the following primers: forward primer, 5'-AACCTCCTCCTCATCGTACT-3', reverse primer 5'-GACAGCATCAGCCATGTTCA-3'. qRT-PCR analysis was conducted using SuperReal PreMix Plus (Tiangen, China) on an Mx 3000P machine (STRATAGENE, Santa Clara, CA, USA). The PCR reaction included a 25 μ L mixture with 12.5 μ L of SYBR Premix Ex Taq II (Tli RNaseH Plus) (2 \times), 1 μ L of each primer, 3 μ L of cDNA, and 8.5 μ L of dH₂O. The PCR program comprised 40 cycles of 94 $^{\circ}$ C for 30 s, 95 $^{\circ}$ C for 5 s, and 60 $^{\circ}$ C for 60 s. mRNA levels were determined using the $2^{-\Delta\Delta C_t}$ method, and all gene expression experiments were performed in triplicate.

Vectors construction of *NnARF17* and *NnARF18*

NnARF17 and *NnARF18* were integrated into the pGEM-T vector and introduced into *Escherichia coli* for replication. Utilizing *Bam*HI and *Kpn*I enzymes, the recombinant forms of these genes were digested to isolate the targeted genes with specific restriction enzyme sites. The plant transformation vector pSN1301, featuring a CaMV 35 S promoter, was selected to

create pSN1301::*NnARF17* and pSN1301::*NnARF18*, subsequently transferred into *Agrobacterium tumefaciens* strain GV3101 for *Arabidopsis* plant preparation. The floral dip method, as described by Clough et al. [36], was employed in this experiment.

Generation of transgenic *Arabidopsis* plants

Seeds of the T0 generation were initially screened on Murashige and Skoog (MS) medium supplemented with 20 μ g/g hygromycin B to identify “positive” plants. Subsequently, these plants were transferred to a greenhouse for continuous cultivation at 22 $^{\circ}$ C (12 h/light and 12 h/dark). qRT-PCR was conducted to further confirm the identity of “positive” plants during the cultivation period, using the same PCR mixture and program as employed for gene cloning.

Functional analysis of *NnARF17* and *NnARF18* on root formation.

Gene functionality was assessed at the six-leaf stage in transgenic *Arabidopsis* plants, with wild-type plants serving as controls. To explore their impact on root formation and plant growth, both transgenic and wild-type plants were subjected to sterilization with 80% alcohol for 20 s, followed by a 10% sodium hypochlorite treatment for 20 min. Sterilized seeds from both plant types were then placed on MS medium and a base material composed of soil and vermiculite in a 1:1 ratio (v/v).

Subcellular localization of *NnARF17* and *NnARF18* in tobacco plants

Tobacco (*Nicotiana tabacum* L.) seeds underwent initial sterilization before being sown in soil for germination at 26 $^{\circ}$ C in the dark. Upon reaching the eight-leaf stage, seedlings were transferred to an illuminating incubator, alternating between 26 $^{\circ}$ C for 12 h in the light and 22 $^{\circ}$ C for 12 h in the dark.

Recombinant plasmids of *NnARF17*, *NnARF18* and *pCAMBIA1300-35 S-EGFP* (expressing vector) were digested by *Bam*HI and *Xba*I enzymes for about 2 h in a water bath pot under 37 $^{\circ}$ C condition. DNA gel recovery kit (TaKaRa, Kusatsu, Japan) was used to obtain fragments of these two genes and expressing vector according to instruction of the Kit. *NnARF17* and *NnARF18* were inserted into *pCAMBIA1300-35 S-EGFP* by T4 DNA ligase at 16 $^{\circ}$ C for 12 h. Recombinant plasmids of *NnARF17*, *NnARF18* were identified by PCR method and double enzymes' digestion.

pCAMBIA1300-35 S-EGFP::NnARF17 and *pCAMBIA1300-35 S-EGFP::NnARF18* were introduced into *A. tumefaciens* (GV3101) through electroconversion, followed by a 2-day incubation at 30 $^{\circ}$ C. *A. tumefaciens* was harvested from the solid medium, suspended in 10 mL of YEB liquid medium, and incubated at 170 rpm/min for 1 h. After centrifugation at 4,000 rpm for 4 min,

the supernatant was discarded, and the precipitate was resuspended in 10 mM MgCl₂ to achieve an OD₆₀₀ of 0.6. Using a 1 mL syringe without a nozzle, the lower epidermis of tobacco leaves was injected. The injected plants were cultured under low-intensity light for 2 days. Labeled leaves were placed on glass slides and observed under a laser confocal microscope.

Analysis of RNA sequencing data

RNA sequencing analysis for NnARF17 and NnARF18

The seeds of both transgenic and wild-type plants underwent sterilization before germinating on base materials at 26 °C. Subsequently, germinated seeds were transferred to a greenhouse for continuous cultivation, maintaining an average temperature of 23±2 °C under 12 h/light and 12 h/dark conditions.

For genome-wide gene expression analysis, RNA sequencing (RNA-seq) was conducted when the seedlings reached the six-leaf stage. Approximately 2–3 µg of total plant RNA from both transgenic and wild-type plants was extracted for constructing libraries (control library, *NnARF17* library, and *NnARF18* library). Library construction followed the procedure described by Cheng et al. [35], and the libraries were sequenced by Nanjing Jisi Huiyuan Biotechnology Co., Ltd. (Nanjing, China).

Annotation of differentially expressed genes

The genome-wide gene expression data from each library underwent a parallel comparison using Illumina sequencing platforms. Subsequently, differentially expressed genes (DEGs) were identified using the NOISeq method, as outlined by Cheng et al. [21]. A fold change in expression ≥2 and a divergence probability ≥0.8 were set as the thresholds for DEG identification.

To elucidate the functional aspects of these DEGs, gene annotation was performed using the Gene Ontology (GO) tool. DEGs were categorized into three ontologies—molecular function, cellular components, and biological processes—based on the instructions provided by the GO tool. Enrichment analysis was conducted by comparing DEGs with the *Arabidopsis* genome obtained from the NCBI database, utilizing a hypergeometric test to determine significantly enriched GO terms. Furthermore, all DEGs were classified into various biological pathways through enrichment analysis, comparing them with the NCBI database genome, and utilizing the Kyoto Encyclopedia of Genes and Genomes.

Determination of IAA, ABA, GA3, peroxidase, polyphenol oxidase, and IAAO content

The seeds of transgenic (*NnARF17* and *NnARF18*) and wild-type *Arabidopsis* plants were sown on base material and placed in an illuminating incubator at 22 °C. The determination of IAA, ABA, GA3, and peroxidase (POD)

contents occurred when the plants reached the six-leaf stage. Additionally, lotus seed coats were broken and subjected to water for germination at 26 °C. Seedlings treated with 10 µM IAA for 2 days were then transferred into water for continuous cultivation. Five time points (0, 2, 4, 6, and 8 days) were selected for the analysis of IAA, GA3, ABA, POD, polyphenol oxidase (PPO), and IAAO contents.

Samples were initially flash-frozen in liquid nitrogen and ground into powder using a rod. Approximately 3 g of powder from transgenic and wild-type plants were utilized for the extraction of IAA, ABA, and GA3. In a centrifuge tube, 600 µL of a reagent composed of isopropyl alcohol, water, and concentrated hydrochloric acid (2:1:0.002, v/v/v) was combined with the sample and agitated at 4 °C for 30 min. The resulting mixture underwent centrifugation at 12,000 rpm at 4 °C for 10 min. The supernatant was discarded, and the precipitate was collected, dried with nitrogen, and dissolved in filtered methanol (50 mL). The solution was then analyzed for IAA and ABA contents using a liquid chromatograph (Sigma, Shanghai, China) [37, 38]. The GA3 content was determined following the method outlined by Nhujak et al. [39]. For the determination of POD, PPO, and IAAO contents, 0.1 g of freeze-dried sample was homogenized in 1 mL of extraction solution in an ice bath. After centrifugation at 8,000 rpm at 4 °C for 10 min, the supernatant was used for subsequent experiments. Each sample was added to a 1 mL glass colorimetric dish, and absorbance values at 470, 410, and 530 nm were measured to quantify POD, PPO, and IAAO, respectively. These experiments were conducted in triplicate.

Stress tolerance of transgenic and wild-type plants

Approximately 100 seeds of both transgenic and wild-type plants were soaked in water for 48 h and then transferred to a medium (v/v, soil: vermiculite=1:1) at 22 °C. Seedlings at the six-leaf stage were employed to evaluate waterlogging, drought, and salt tolerance. For waterlogging analysis, transgenic and wild-type plants were placed in a tray with water at a depth of 2 cm for approximately 20 days, followed by transfer to normal growth conditions. Measurements of fresh weight, dry weight, and stem growth were taken after 10 days of cultivation. To assess drought tolerance, both types of plants were initially grown under identical water management conditions, and then water was withheld for about 10 days. The survival rates of the plants were determined after 7 days of water recovery. For salt tolerance assessment, transgenic and wild-type plants were treated with 100 mM NaCl, and the survival rates were evaluated after approximately 10 days. Three biological replicates were utilized for each type of plant, and each replicate involved at least 50 seedlings.

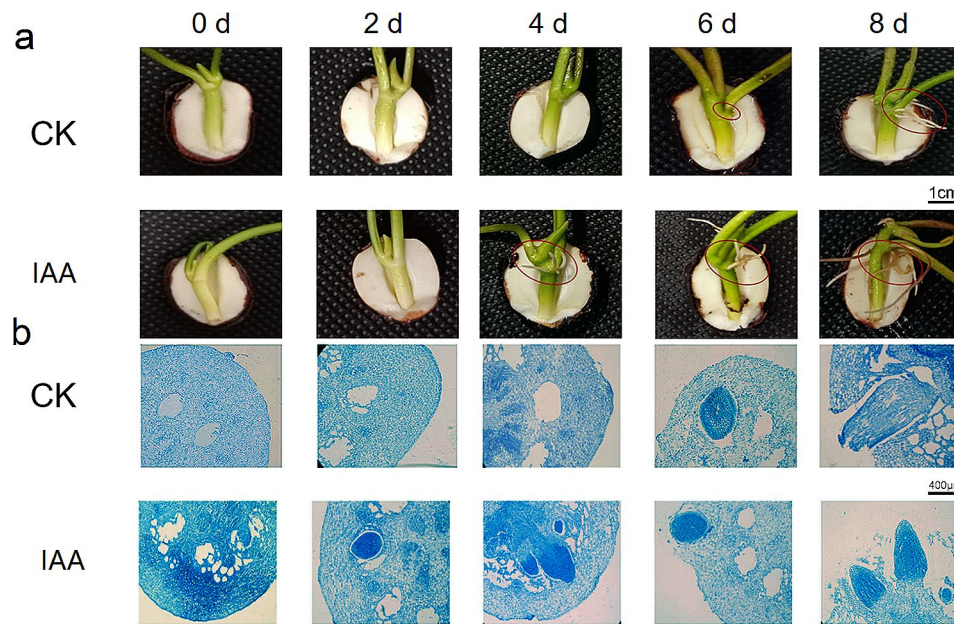


Fig. 1 The role of exogenous application of IAA on ARs formation in lotus seedlings. **a**. Observation of root growth from morphology of seedlings treated with 10 μ M IAA for 0 d, 2 d, 4 d, 6 d, and 8 d. Analysis of microstructure on ARs formation at the hypocotyls of lotus seedlings treated with 10 μ M IAA for 0 d, 2 d, 4 d, 6 d, and 8 d. Ellipses represents ARs or ARs primordium

Table 1 Expression changes of genes involved in IAA metabolism, response and root formation in transgenic *NnARF17*, *NnARF18* and wild type *Arabidopsis* plants

| ID | <i>NnARF17</i> | <i>NnARF18</i> | Function annotation |
|---|----------------|----------------|---|
| Genes involved in hormone metabolism and signal transduction pathway | | | |
| AT1G15520 | 1.13 | ----- | Pleiotropic drug resistance 12 |
| AT1G32630 | -1.32 | ----- | Transcription factor MYC2 |
| AT2G44840 | -1.76 | ----- | Ethylene-responsive element binding factor 13 |
| AT4G03585 | ----- | 4.11 | Cytochrome P450 |
| AT2G20880 | ----- | 2.32 | Ethylene-responsive transcription factor ERF053 |
| AT2G36270 | ----- | -1.01 | bZIP transcription factor family protein |
| Genes involved in root formation | | | |
| AT1G15000 | 9.54 | ----- | Serine carboxypeptidase-like 50 |
| AT4G38860 | 1.01 | ----- | SAUR-like auxin-responsive protein family |
| AT4G27260 | -1.21 | ----- | Auxin-responsive GH3 family protein |
| AT3G62090 | -2.69 | ----- | Phytochrome interacting factor 3-like 2 |
| AT3G18710 | -1.59 | ----- | Plant U-box 29 |
| AT5G10250 | ----- | 1.28 | Phototropic-responsive NPH3 family protein |
| AT2G34060 | ----- | 1.11 | Putative peroxidase |

Note: "-----" represented no changes of expression

Statistical analysis

Statistical analyses were conducted using Origin Pro software (version 8.0; Origin Inc., Framingham, MA, USA). Each experiment was carried out in triplicate, and the means \pm standard errors of the three repetitions were calculated. All figures display mean values with standard errors. Student's t-tests were employed to determine significant differences, with differences considered significant at $p < 0.05$.

Results

IAA influence on lotus AR development

To assess the impact of IAA on lotus AR formation, seedlings underwent a 2-day treatment with 10 μ M IAA. The results demonstrated that IAA treatment significantly enhanced AR development, with ARs breaking through the hypocotyl epidermis after 4 days, while control plants required 6 days for AR appearance (Fig. 1a). Concurrently, microstructural analysis revealed clear induction and development of AR primordia after 2 days, with visible ARs in the hypocotyl after 4 days in treated seedlings (Fig. 1b). In contrast, control plants exhibited a longer duration for complete AR formation. These findings indicate that IAA expedites the AR formation process, particularly during the induction stage in lotus seedling hypocotyls.

Cloning and sequences analysis of *NnARF17* and *NnARF18*

In a prior investigation, we observed the induction of two sucrose-responsive auxin genes significantly promoting

AR formation in lotus seedlings. Subsequently, these genes were cloned using RT-PCR, resulting in open reading frames of 1,797 and 2,052 bp for *NnARF17* and *NnARF18*, respectively. These encoded proteins of 599 and 684 amino acid residues (Additional Table 1; Fig. 2a). Comparative analysis with data from the NCBI database revealed the presence of conservative domains in *ARF17* and *ARF18* encoding proteins in *Camellia*, *Macadamia*, *Theobroma*, and *Prunus* (Additional Figs. 1 and 2), leading to their designation as *NnARF17* and *NnARF18*. Despite having low sequence similarity, both *NnARF17* and *NnARF18* contained identical auxin response and B3 homeobox elements (Fig. 2a and b). Furthermore, examination of protein domains indicated their similarity, hinting at potential shared biological functions (Fig. 2c). Phylogenetic analysis identified 11 groups, with *NnARF17* forming an independent group (group 6), highlighting its distant relationship with members of other groups. In contrast, *NnARF18* showed close associations with *BvARF18*, *CpARF18*, *ZjARF18*, *GhARF18*, *PtARF18*, and *JcARF18*, placing them in a shared group (Fig. 2d).

qRT-PCR analysis in *NnARF17* and *NnARF18*

The transcriptional profiles of *NnARF17* and *NnARF18* were scrutinized through qRT-PCR, providing consistent results with those obtained through alternative methods. *NnARF17* exhibited similar expression patterns in seedlings treated with IAA, ethephon, and sucrose, with mRNA levels peaking after 2 days of water cultivation. In contrast, *NnARF18* though induced by IAA, ethephon, and sucrose, displayed a distinct expression

trend compared to *NnARF17*. Tissue-specific expression patterns of *NnARF17* and *NnARF18* were investigated across various organs, revealing distinctive preferences. The highest transcription levels were observed in fruits, followed by ARs, stems, leaves, and flowers. Notably, *NnARF18* exhibited higher expression in ARs compared to other organs (Fig. 3).

Subcellular localization of *NnARF17* and *NnARF18*

In-depth subcellular localization assays were executed to precisely determine the functional gene locations of *NnARF17* and *NnARF18* within tobacco organelles. The instantaneous transfer of *NnARF17* and *NnARF18* to tobacco plants at the eight-leaf stage was performed, with *35 S::empty vector GFP* serving as the control. The fluorescence signals for GFP were notably robust and evident in the merged field, displaying clear contours in the bright field. *NnARF17* and *NnARF18* exhibited similar localization patterns within tobacco plants, with both genes primarily situated in the nuclei on their positions in plant cells (Fig. 4). This localization strongly suggests that *NnARF17* and *NnARF18* function as nuclear genes, influencing root formation in transgenic *Arabidopsis* plants.

Root development in transgenic *Arabidopsis* plants

Successful construction of *pSN1301:NnARF* and *pSN1301:NnARF18* paved the way for investigating the roles of these genes in root formation using transgenic *Arabidopsis* plants. Identification of “positive” plants was achieved through PCR analysis. Notably, transgenic

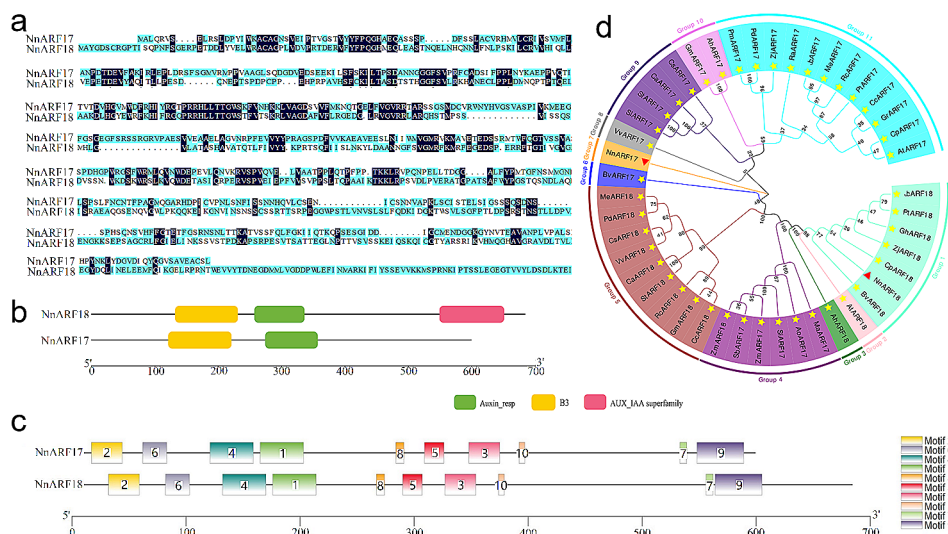


Fig. 2 Comparison and phylogenetic tree analysis of *NnARF17* and *NnARF18*. **(a)** Comparison of *NnARF17* and *NnARF18* with amino acid sequences. **(b)** Domain analysis of *NnARF17* and *NnARF18* encoded proteins, and the box different color represents conserved region. **(c)** Motifs analysis of *NnARF17* and *NnARF18* encoded proteins. Boxes of different colors represent the ten putative motifs, and the boxes with the same color represent the same motif in structure of these three genes. **(d)** Phylogenetic tree analysis of *NnARF17* and *NnARF18* encoded proteins with *ARF17* and *ARF18* encoded protein of other species, and total eleven groups with different color were detected. The red triangle represents the positions of the *NnARF17* and *NnARF18* encoded proteins in the phylogenetic tree

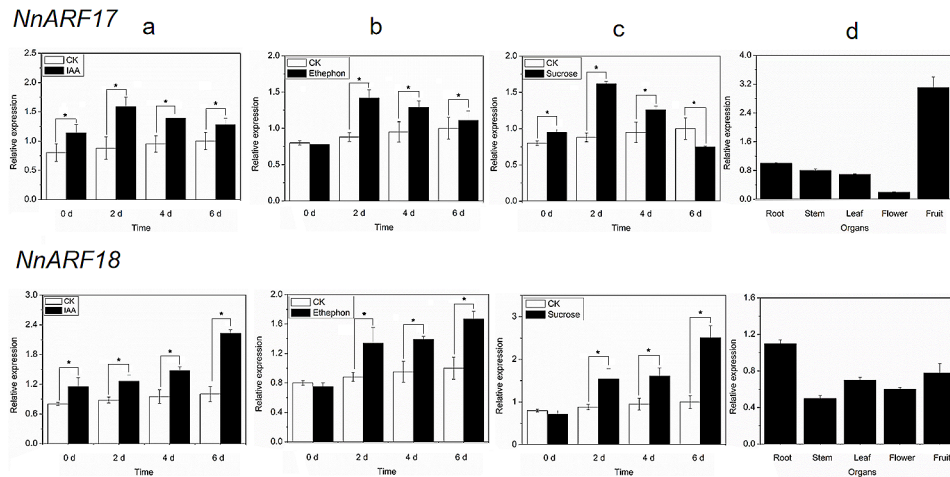


Fig. 3 Expression patterns of *ARF17* and *ARF18* with different treatments and in different organs, as determined by qRT-PCR. **(a)** Expression analysis of *NnARF17* and *NnARF18* after IAA treatment. **(b)** Identification of *NnARF17* and *NnARF18* expression in lotus seedlings treated with ethephon. **(c)** Determination of *NnARF17* and *NnARF18* expression in lotus seedlings treated with sucrose. **(d)** Organ-specific expression analysis in roots, stems, leaves, flowers and fruit of lotus plants. The data were recorded as means \pm SEs of three biological replicates with about five seedlings in each experiment. Significant differences were carried out and determined by presented as * $p < 0.05$

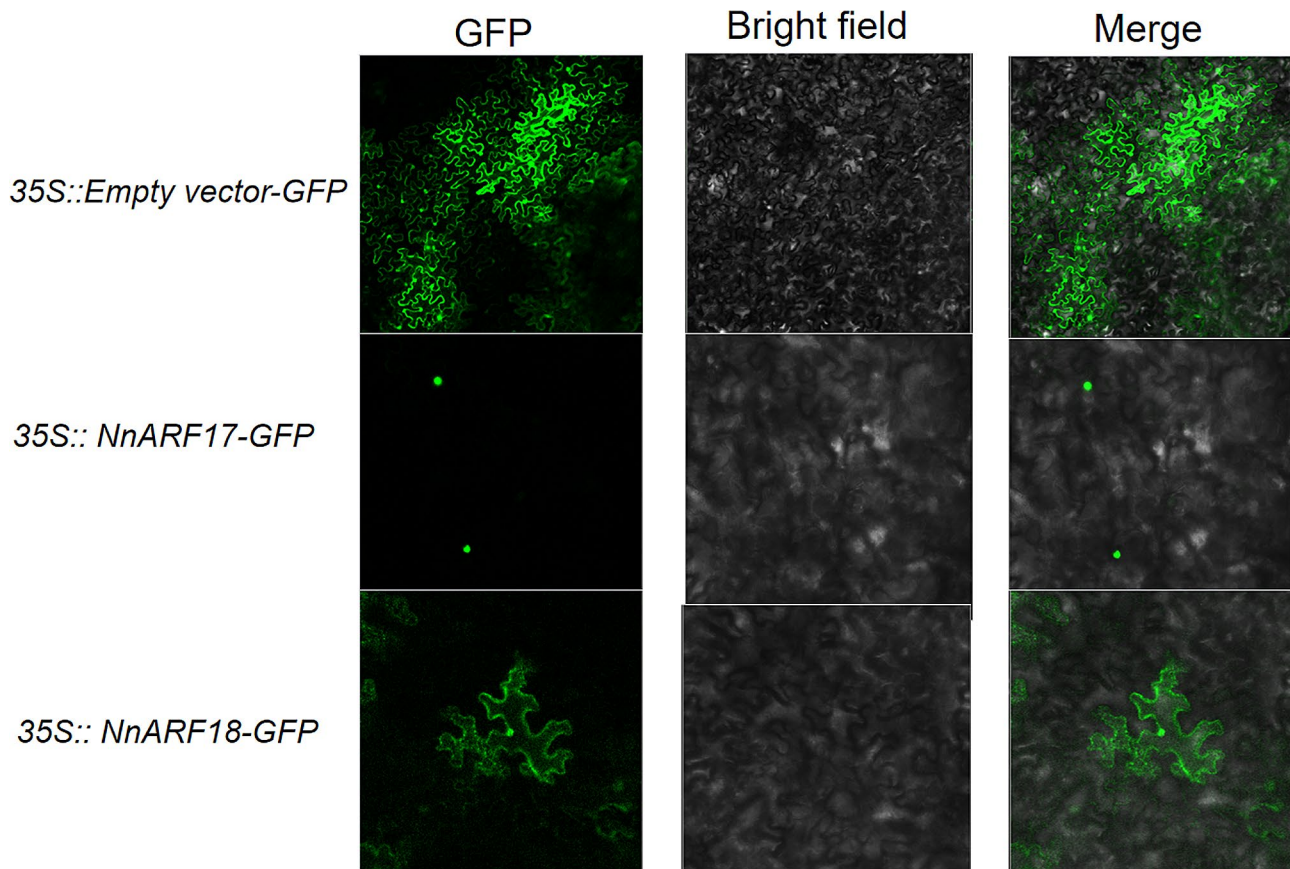


Fig. 4 Subcellular localization of *NnARF17* and *NnARF18* in tobacco plants

plants expressing *NnARF17* and *NnARF18* exhibited significantly longer roots and a higher abundance of roots compared to wild-type plants, as illustrated in Fig. 5a and c. Furthermore, the influence of *NnARF17* and *NnARF18*

extended to stem growth, with *Arabidopsis* plants displaying constitutive expression of these genes showcasing elevated stem heights in comparison to wild-type plants (Fig. 5b and c). These findings underscore the

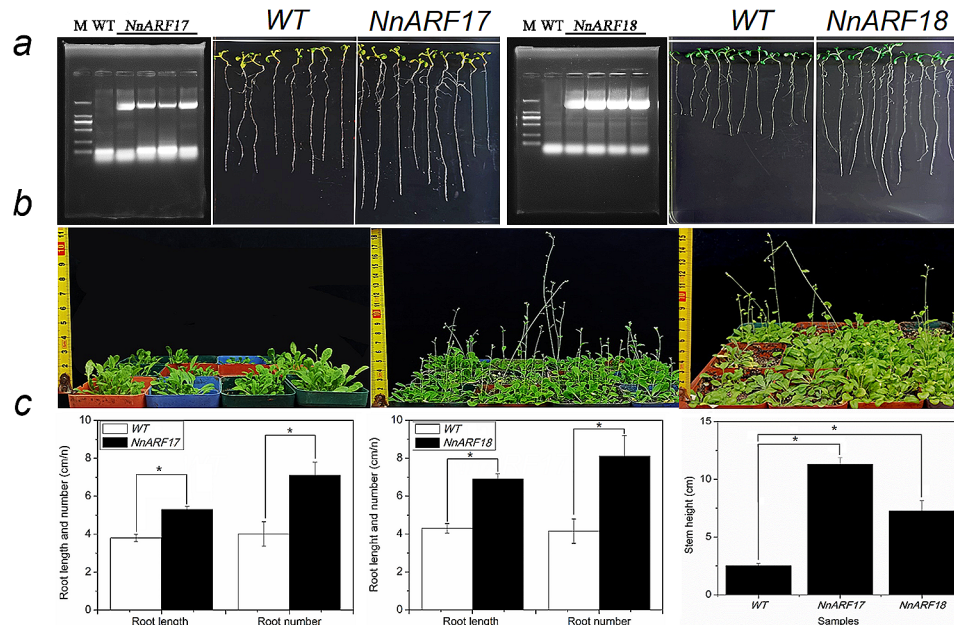


Fig. 5 Functional analysis of *NnARF17* and *NnARF18* in transgenic *Arabidopsis* plants. **(a)** Assessment of root development in transgenic plants with constitutive *NnARF17*, *NnARF18* and wild-type plants. **(b)** Effect of *NnARF17* and *NnARF18* on stem growth in transgenic *Arabidopsis* plants. **(c)** Statistic analysis of *NnARF17* and *NnARF18* role on root and stem development. The mean values were calculated from three replicated experiments, and error bars showed standard deviation. Significant differences were determined by Student's t-test. Statistically significant difference between two samples was presented as * $p < 0.05$

involvement of *NnARF17* and *NnARF18* in diverse biological processes within transgenic *Arabidopsis* plants.

Analysis of gene expression in transgenic and wild-type *Arabidopsis* plants

At the five-to-six-leaf stage, both transgenic and wild-type plants were scrutinized for alterations in gene expression through RNA-seq analysis. The results unveiled distinct transcriptional changes in transgenic plants, with 51 genes, including eight upregulated and 43 downregulated genes, exhibiting modified expression levels in transgenic *NnARF17* plants. Similarly, transgenic *NnARF18* plants displayed changes in 75 genes, comprising 26 upregulated and 49 downregulated genes (Fig. 6a).

Comparative analysis revealed that only six genes were implicated in the same biological pathways in both transgenic plants (Fig. 6b). Further exploration of these DEGs pinpointed five genes associated with plant hormone metabolism and signal transduction. Noteworthy candidates included pleiotropic drug resistance 12, SAUR-like auxin-responsive protein family, auxin-responsive GH3 family protein, transcription factor MYC2, ethylene-responsive element binding factor 13, cytochrome P450, ethylene-responsive transcription factor ERF053, and bZIP transcription factor family proteins (Fig. 6c and d; Table 1). Seven genes linked to root formation exhibited altered expression levels (Table 1).

Additionally, scrutiny of stress response-related genes unveiled noteworthy changes. In transgenic *NnARF17* plants, three genes (stress response component-like protein, serine carboxypeptidase-like 50, and NAC domain-containing protein 1) were upregulated, while six genes (stress response component-like protein, plant U-box 29, serine carboxypeptidase-like 50, transcription factor MYB15, transcription factor MYB90, and xyloglucan endotransglucosylase) were downregulated. In transgenic *NnARF18* plants, seven genes (F-box/kelch-repeat protein SKIP6, E3 ubiquitin-protein ligase, glutathione S-transferase U2, NAC domain-containing protein 1, putative POD, fatty acid desaturase 8, and multidrug resistance protein/P-glycoprotein-like) exhibited increased expression levels, while five genes (basic-leucine zipper [bZIP] transcription factor family protein, WRKY DNA-binding protein 45, basic helix-loop-helix [bHLH] DNA-binding superfamily protein, calcium ion-binding protein, and U-box kinase family protein) showed decreased expression levels (Table 2).

Determination of IAA, ABA, GA3, and POD contents in transgenic *Arabidopsis* plants

Given the pivotal roles of IAA, ABA, GA3, and POD in lotus seedling AR formation, we conducted an analysis of these substances in transgenic *Arabidopsis* plants. The results unveiled a notable decrease in IAA content in both transgenic *NnARF17* and *NnARF18* plants compared to wild-type plants, implying a discernible impact

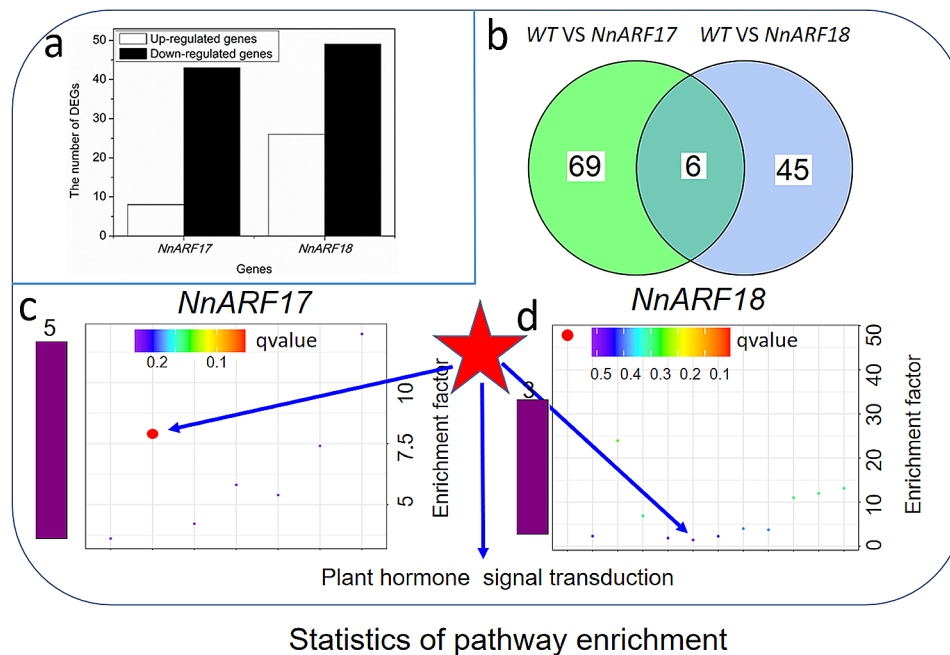


Fig. 6 Statistical analysis of DEGs and pathway enrichment in transgenic plants. **(a)** Number of DEGs following overexpression of *NnARF17* and *NnARF18* in *Arabidopsis* plants. **(b)** Distribution of DEGs between *NnARF17* and *NnARF18* transgenic plants. **(c)** Genes involved in plant hormone transduction pathway are counted in transgenic plants expressing *NnARF17* and *NnARF18*.

of *NnARF17* and *NnARF18* on IAA metabolism. Furthermore, the ABA content exhibited a significant increase in these transgenic plants, while GA3 and POD content remained unchanged when juxtaposed with wild-type plants (Fig. 7).

To delve deeper, we examined the expression of genes pertinent to IAA metabolism and observed an elevated expression level of pleiotropic drug resistance 12, a member of the ATP-binding cassette superfamily, implicated in auxin transport (Table 1). The precise relationship between the reduced IAA content in transgenic plants and the upregulation of this gene warrants further investigation.

Adaptation of transgenic *Arabidopsis* plants to waterlogging, drought, and salt stress

To unravel the roles of *NnARF17* and *NnARF18* in plant adaptation to adverse conditions, we subjected transgenic plants overexpressing these genes, along with wild-type plants, to waterlogging, drought, and salt stress. The outcomes revealed that transgenic plants exhibited lower survival rates, decreased fresh and dry weights, and shorter stems under waterlogging conditions compared to wild-type plants, indicating reduced adaptation to waterlogging in plants constitutively expressing *NnARF17* and *NnARF18* (Fig. 8a). Interestingly, these transgenic plants displayed enhanced tolerance to drought stress compared to the wild type (Fig. 8b). However, no significant difference was observed between

transgenic and wild-type plants under salt stress conditions (Fig. 8c).

In summary, *NnARF17* and *NnARF18*, primarily associated with root formation, exhibit a strong correlation with stress adaptation in transgenic *Arabidopsis*.

Changes in physiological indices in lotus seedlings after IAA treatment

To assess the impact of 10 μ M IAA treatment over 2 days on lotus seedlings, we monitored changes in IAA, GA, ABA, IAAO, PPO, and POD content. Notably, the IAA content exhibited a marked decrease from day 0 to day 6 after IAA treatment. The GA3 content initially increased, followed by a significant decrease. The ABA content consistently increased from day 0 to day 8, surpassing the levels observed in control plants. In the context of AR formation, the POD content displayed dynamic changes over the 8-day period: an initial increase from day 0 to 2, followed by a decrease from day 2 to 6, and a subsequent increase on day 8 (Fig. 9a). Further scrutiny of the two enzymes associated with IAA metabolism revealed that the IAAO content exhibited a continuous increase from day 0 to 6, followed by a decrease on day 8. Conversely, the PPO content in treated seedlings decreased from day 0 to 6 and then increased on day 8 (Fig. 9b).

Discussion

ARs play a vital role in nutrient and water absorption in lotus plants, particularly in light of the underdevelopment of primary roots. These ARs are subject to various

Table 2 Expression of genes related to stresses response in transgenic *NnARF17* and *NnARF18* *Arabidopsis* plants

| ID | <i>NnARF17</i> | <i>NnARF18</i> | Function annotation |
|-----------|----------------|----------------|---|
| AT4G39840 | 12.34 | ----- | Stress response component-like protein |
| AT1G15000 | 9.54 | ----- | Serine carboxypeptidase-like 50 |
| AT1G01010 | 1.7 | 1.62 | NAC domain-containing protein 1 |
| AT4G39838 | -1.28 | ----- | Stress response component-like protein |
| AT3G18710 | -1.59 | ----- | Plant U-box 29 |
| AT1G15002 | -1.76 | ----- | Serine carboxypeptidase-like 50 |
| AT3G23250 | -2.92 | ----- | Transcription factor MYB15 |
| AT1G66390 | -2.93 | ----- | Transcription factor MYB90 |
| AT4G30280 | -3.63 | ----- | Xyloglucan endotransglucosylase |
| AT2G07475 | ----- | 3.60 | F-box/kelch-repeat protein SKIP6 |
| AT1G66040 | ----- | 2.62 | E3 ubiquitin-protein ligase |
| AT2G29480 | ----- | 1.76 | Glutathione S-transferase U2 |
| AT2G34060 | ----- | 1.18 | Putative peroxidase |
| AT5G05580 | ----- | 1.03 | Fatty acid desaturase 8 |
| AT4G18050 | ----- | 1.00 | Multidrug resistance protein/P-glycoprotein-like |
| AT2G36270 | ----- | -1.01 | Basic-leucine zipper (bZIP) transcription factor family protein |
| AT3G01970 | ----- | -1.25 | WRKY DNA-binding protein 45 |
| AT4G28790 | ----- | -1.89 | Basic helix-loop-helix (bHLH) DNA-binding superfamily protein |
| AT2G04755 | ----- | -5.35 | Calcium ion-binding protein |
| AT3G61410 | ----- | -2.24 | U-box kinase family protein |

Note: "-----" represented no changes of expression

factors directly influencing plant growth and environmental adaptation. Our study revealed a significant promotion of AR development in lotus seedlings treated with 10 μ M IAA (Fig. 1a). The role of IAA has garnered extensive attention in recent research, with implications in diverse biological processes, such as growth, development, and stress adaptation, despite its low plant content. At the cellular level, auxin, including IAA, regulates plant cell division, elongation, and differentiation [11, 12]. On the organ scale, auxin contributes to the formation of various organs, including roots, buds, leaves, flowers, and fruits [13, 14]. Additionally, auxins play a crucial role in vascular tissue differentiation and plant tropisms, such as gravitropism and phototropism [9, 40]. Specifically, auxin is implicated in root cap development and fosters root formation during AR initiation [15, 16]. Exogenous IAA, as demonstrated in our study, significantly enhances cell division and primordium formation, accelerating the development of AR primordia compared to control plants. This suggests that IAA regulates the initial

stage of AR formation (induced stage), prompting further investigation into its impact on the initiation and expression stages of AR development in lotus plants (Fig. 1b).

ARFs play crucial roles as either activators or repressors in plant growth and development, impacting processes like root initiation, apical dominance, tropism, and cellular functions. This extensive family, comprising numerous members [41], has been identified in various species, albeit with varying family sizes [42]. As pivotal transcription factors, ARFs regulate downstream gene expression by binding to auxin response elements in promoters with a consensus sequence [43, 44]. Generally, AUXs/IAAs represent domains within ARFs responsive to auxin stimulation [45]. Furthermore, despite low sequence similarity in the encoding proteins, the B3 domain remains a conserved structure in ARF family members [46, 47].

In our prior study, *NnARF17* and *NnARF18* were found to be upregulated in lotus seedlings following sucrose treatment [34]. In the current investigation, we successfully cloned *NnARF17* and *NnARF18*. Sequence analysis revealed limited homology between the encoded proteins of *NnARF17* and *NnARF18*. However, these proteins shared identical domains (Fig. 2a, b, and c). This phenomenon, also observed in *Salix suchowensis*, where many ARFs exhibit similar expression profiles during different growth stages [48], suggests a connection between this pattern and protein structure. Phylogenetic analysis further supported this hypothesis, placing *NnARF17* and *NnARF18* in distinct groups despite sharing domains and motifs (Fig. 2d). Remarkably, *NnARF17* and *NnARF18* exhibited analogous expression profiles, being induced by IAA, sucrose, and ethephon (Fig. 3). This suggests that despite sequence differences, these genes might not differ significantly in their regulation of plant metabolism.

Auxins play a crucial role in the physiological process of AR formation by orchestrating the expression of downstream genes [49]. In our study, the overexpression of auxin-induced genes, namely, *NnARF17* and *NnARF18*, was found to significantly promote root formation in transgenic *Arabidopsis* plants (Fig. 4). Numerous key genes are known to be involved in the IAA response, with transport and synthesis playing pivotal roles in AR developmental processes [50, 51]. For instance, ARF6, ARF8, and ARF17 have been identified as contributors to AR development [52].

In the early auxin response, three genes—auxin, *GH3*, and *SAURs*—are rapidly activated by auxin [53]. We observed a downregulation of *GH3* in the transgenic *Arabidopsis* plants (Table 1). *GH3*, responsible for synthesizing jasmonic acid and IAA, plays a role in jasmonic acid- and salicylic acid-mediated plant defense reactions and photoreactions [53]. Notably, *GH3* mutants have been associated with enhanced development of main and lateral roots [43], suggesting that changes in *GH3*

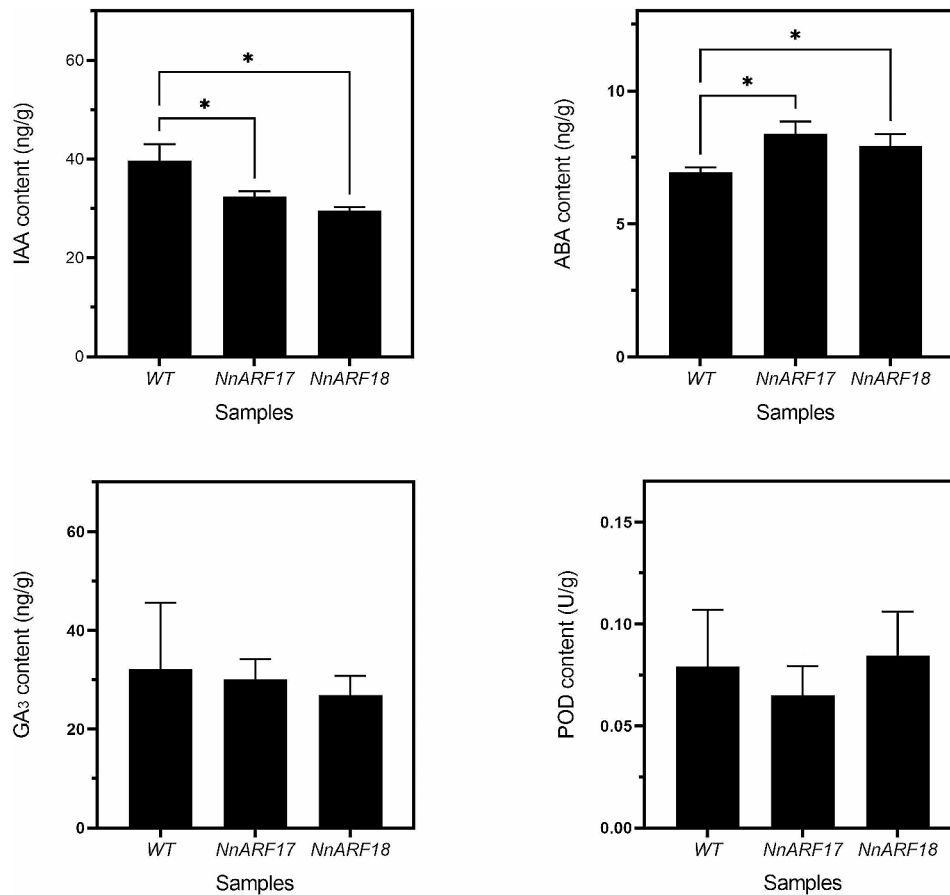


Fig. 7 Determination of IAA, GA₃, ABA, and POD contents in transgenic plants with *NnARF17* and *NnARF18* and in wild-type plants. For statistical analysis, the data were recorded as means ± SEs of three biological replicates with about twenty seedlings in each experiment. Significant differences were determined by Student's t-test. Statistically significant difference between two samples was presented as * $p < 0.05$

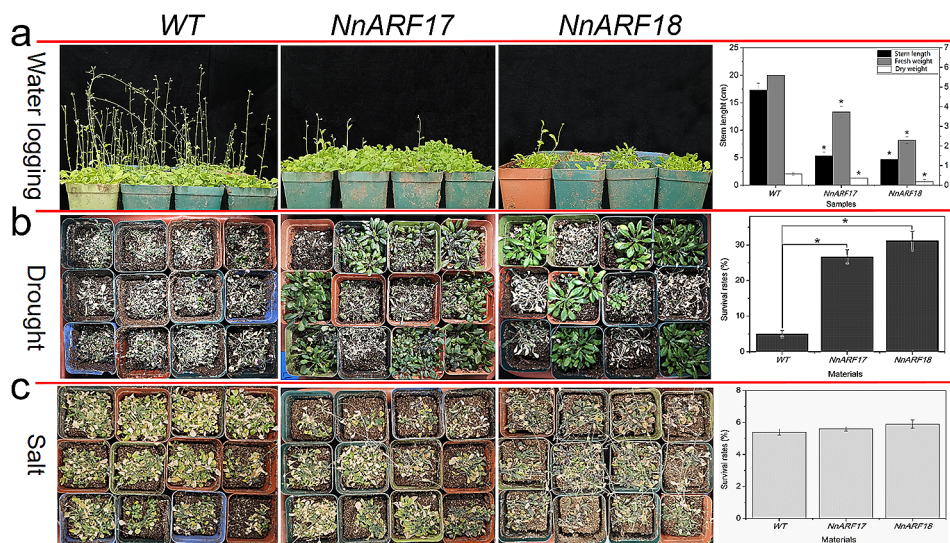


Fig. 8 Survival rates of transgenic *NnARF17* and *NnARF18* plants and wild-type plants in response to waterlogging, drought and salt stresses. **(a)** Survival rates of transgenic *NnARF17*, *NnARF18* and wild type *Arabidopsis* plants after waterlogging treatment. **(b)** Survival rates of transgenic *NnARF17*, *NnARF18* plants and wild-type plants after drought treatment. **(c)** Survival rates of *NnARF17*, *NnARF18* transgenic plants and wild type plants after salt treatment. The data were recorded as means ± SEs of three biological replicates with about fifty seedlings in each experiment. Significant differences were determined by Student's t-test. Statistically significant difference between two samples was presented as * $p < 0.05$

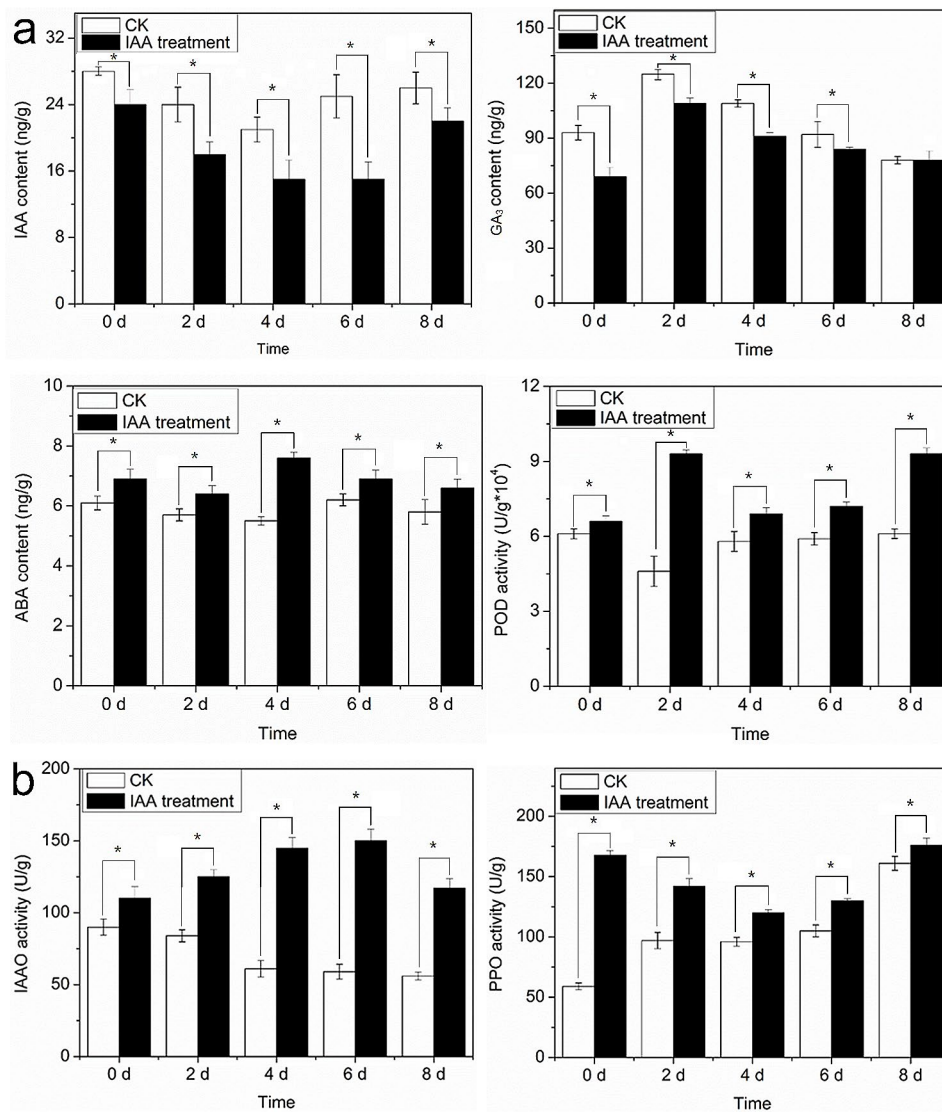


Fig. 9 Role of IAA on the development of lotus seedlings. a. Effect of exogenous IAA on the content of IAA, ABA, GA₃, POD, PPO and IAAO in lotus seedlings at 0, 2, 4, 6 and 8 d after 10 μM IAA treatment. Each experiment was carried out with three replicates, and the data represents means ± SEs for about 20 seedlings. Significant differences were determined by Student's t-test. Significant difference between two samples was presented as * $p < 0.05$

expression levels may influence both root development and stress adaptation.

Auxin transport, involving polar, non-polar, and horizontal modes [54], plays a critical role in root formation. Polar transport, occurring from the upper end to the lower end of plant morphology, has extensive physiological roles, including induction of leaf primordium, differentiation of leaf microtubule structures, and stress responses [55–57]. Non-polar transport involves the rapid micro-diffusion of auxins up and down the plant through the phloem [58]. Horizontal transportation, affected by gravity, light, and internal charge distribution, occurs in roots and stem tips [59].

Two types of IAA transporters, influx and efflux carriers, have been identified to date. The AUX1/LAX family,

categorized as influx carriers, significantly influences root development by triggering IAA distribution [60, 61]. Our findings indicate that plants with constitutive expression of *NnARF18* exhibit enhanced expression of a gene associated with polar auxin transport. Furthermore, the transcription level of an auxin-responsive gene increases with *NnARF18* overexpression (Fig. 5; Table 1), highlighting the critical role of auxin transport in root formation.

In addition to the recognized positive roles of IAA and ethylene, ABA signaling emerges as a crucial player influencing AR development [22, 62, 63]. Subsequent studies have delved into the nuanced impact of ABA on AR formation, revealing its inhibitory effect primarily during the induction stage of primordium and root elongation stages in softwood cuttings. Interestingly, ABA/IAA is

found to be beneficial for the induction of root primordium [23]. ABA exerts its influence on AR formation by augmenting the accumulation and activity of endogenous IAA [64]. Moreover, ABA demonstrates its multifaceted impact by inhibiting the rate of AR growth through modulation of GA biosynthesis and activity, coupled with IAA signaling in rice [24]. Therefore, the ABA / (IAA+GA3) ratio emerges as a valuable indicator of rooting capacity [25].

Intriguingly, our study revealed a novel facet of ABA's involvement in AR development by enhancing the content of photosynthates, including glucose, sucrose, starch, total sugars, glucose-6-phosphate, fructose-6-phosphate, and glucose-1-phosphate [62]. This aligns with findings in cucumbers, where an intricate interplay between ABA and glucose regulates AR formation, and ABA, in turn, promotes AR development by elevating endogenous ABA accumulation [63].

Our experimental evidence further supports the notion that plants overexpressing *NnARF17* and *NnARF18* exhibit a significant increase in ABA content (Fig. 7), and this observation is corroborated by additional experiments involving lotus seedlings treated with IAA, where ABA content also experiences an upswing (Fig. 8). This suggests a potential positive role of ABA in root formation in both transgenic plants and lotus seedlings. Notably, while there was no discernible change in GA3 content in transgenic *Arabidopsis* plants, a significant increase in GA3 content was observed in lotus seedlings treated with IAA.

IAAO, PPO, and POD emerge as pivotal players intricately linked to the intricate process of AR formation in plants. Among these, POD, a key enzyme in lignin synthesis, plays a crucial role in the initiation and elongation of ARs [65]. Comprising various isoenzymes with diverse physical and chemical properties, POD's association with plant root formation has been extensively explored, primarily focusing on organogenesis [7, 66, 67]. Our experimental data unveil a significant surge in POD content in seedlings post IAA treatment, underscoring the potential importance of POD in lotus AR formation (Fig. 8).

IAAO and PPO contribute to the regulation of IAA content in plants by degrading IAA, thereby influencing overall plant growth and development. PPO, a plant-exclusive enzyme, catalyzes the condensation of phenols and IAA, forming an "IAA phenolic acid complex" conducive to AR formation. By catalyzing auxin metabolism, PPO promotes the occurrence and development of ARs, with exogenous hormone application amplifying PPO levels and consequently enhancing AR formation [68]. Additionally, studies by Ahkami et al. [69] highlight the influence of auxin on endogenous IAA content through the regulation of *GH3* expression in *Petunia hybrida*. Integrating these insights with our experimental findings

(Fig. 7), it becomes evident that the IAA content during root formation is influenced by a complex interplay of multiple factors.

ARFs, known for their roles in stress adaptation, including responses to drought, salt, and low temperatures [70, 71], exhibit their influence in the context of overexpressed *NnARF17* and *NnARF18*. The enhanced survival rates of transgenic *Arabidopsis* plants in response to drought (Fig. 8) coincide with an observed increase in ABA content in plants with constitutive expression of these genes (Fig. 7). ABA, recognized for its extensive responsiveness to various stressors [72, 73], prompts further exploration into whether *NnARF17* and *NnARF18* bolster plant adaptation by modulating ABA content. The dynamic nature of gene expression serves as a strategic response to environmental conditions, especially adverse factors [74, 75]. The observed alterations in the mRNA levels of various genes (Table 2) suggest their potential involvement in the adaptation to drought stress in transgenic *Arabidopsis* plants. Intriguingly, the overexpression of *NnARF17* and *NnARF18*, while enhancing drought tolerance, paradoxically reduced tolerance to waterlogging, drought, and salt stress. This hints at the intricate interplay between gene regulation, IAA content, and stress tolerance, warranting further investigation into the underlying mechanisms.

Conclusions

This study confirmed the promotive role of IAA in AR formation in lotus seedlings. We identified and assessed two auxin-responsive genes (*ARF17* and *ARF18*) in *Arabidopsis*, revealing low sequence similarity but similar protein structures for *NnARF17* and *NnARF18*. Induction by IAA, ethephon, and sucrose, and expression in various lotus organs characterized these genes. Constitutive expression of *NnARF17* and *NnARF18* positively influenced root and stem development but negatively impacted waterlogging adaptation while increasing drought stress. Transcriptomic analysis using RNA-seq in transgenic *Arabidopsis* plants demonstrated a decrease in IAA content and an increase in ABA content. Additional examination of IAA, ABA, GA3, PPO, IAAO, and POD contents in lotus seedlings treated with exogenous IAA revealed significant increases. In summary, our findings emphasize the indispensable role of IAA in lotus AR formation by regulating downstream responsive genes.

Supplementary Information

The online version contains supplementary material available at <https://doi.org/10.1186/s12870-024-04852-9>.

Supplementary Material 1

Supplementary Material 2

Supplementary Material 3

Supplementary Material 4

Acknowledgements

We extend our thanks to members of the Nanjing Jisi Huiyuan Biotechnology Co., Ltd for their cooperation in obtaining the data during the ARs formation of the lotus by RNA-seq technique. The authors also thank Editage for their editorial assistance.

Author contributions

Cheng L. and Li S. conceived and designed the experiments. Liang S performed the experiments. Zhao C. and Liang S. analyzed the data. Cheng L. and Li S. wrote the text file. All authors have reviewed and approved the final manuscript. All authors reviewed the manuscript.

Funding

This work was supported by the Modern Agricultural Development Project of Jiangsu Province (BE2021333). The funding bodied had no role in the design or performance of any experiments, data analysis, or writing of the manuscript.

Data availability

The material of all the experiment was supported by aquatic vegetable Lab of Yangzhou University. The collection of seed complied with local and national guidelines and permissions of seed were obtained. The detail data has been deposited in NCBI database (Project: PRJNA1047315; WT1, WT 2, WT 3: SRR27065900, SRR27065899, SRR27065898; ARF17-1, ARF17-2, ARF17-3: SRR27065897, SRR27065896, SRR27065895; ARF18-1, ARF18-2, ARF18-3: SRR27065894, SRR27065893, SRR27065892).

Declarations

Ethics approval and consent to participate

We confirm that all the procedures were followed in accordance with the relevant national, international, and institutional guidelines. Consent to participate was not applicable to this study.

Consent for publication

Not applicable.

Competing interests

The authors declare no competing interests.

Received: 23 January 2024 / Accepted: 22 February 2024

Published online: 02 March 2024

References

- Shen-Miller J. Sacred lotus, the long-living fruits of China Antique. *Seed Sci Res.* 2002;14:131–43.
- Ming R, VanBuren R, Liu YL, Yang M, Han YP, Li LT. Genome of the long-living sacred lotus (*Nelumbo nucifera*. Gaertn). *Gen Biol.* 2013;14:R41.
- Liu RX, Chen SM, Jiang JF, Zhu L, Zheng C, Han S, Gu J, Sun J, Li HY, Wang HB, Song AP, Chen FD. Proteomic changes in the base of chrysanthemum cuttings during adventitious root formation. *BMC Genomics.* 2013;14:919.
- Borgi W, Ghedira K, Chouchane N. Anti-inflammatory and analgesic activities of zizyphus lotus root barks. *Fitoterapia.* 2007;78:16–9.
- Zobel RW, Waisel Y. A plant root system architectural taxonomy: a framework for root nomenclature. *Plant Biosyst.* 2010;144:507–12.
- Kevers C, Hausman JF, Faivre-Rampant O, Evers D, Gaspar T. Hormonal control of adventitious rooting: progress and questions. *J Appl Bot Angewandte Botanik.* 1997;71:71–9.
- Li SW, Xue LG, Xu SJ, Feng HY, An LZ. Mediators, genes and signaling in adventitious rooting. *Bot Rev.* 2009;75:230–47.
- Rasmussen A, Hosseini SA, Hajirezaei MR, Druege U, Geelen D. Adventitious rooting declines with the vegetative to reproductive switch and involves a changed auxin homeostasis. *J Exp Bot.* 2015;66:1437–52.
- Teale WD, Paponov IA, Palme K. Auxin in action: signaling, transport and the control of plant growth and development. *Nat Reviews Mol Cell Biol.* 2006;7:847–59.
- E ZG, Ge L, Wang L. Molecular mechanism of adventitious root formation in rice. *Plant Grow Reg.* 2012;68:325–31.
- Strader LC, Chen GL, Bartel B. Ethylene directs auxin to control root cell expansion. *Plant J.* 2010;64:874–84.
- Kohli A, Sreenivasulu N, Lakshmanan P, Kumar P. The phytohormone crosstalk paradigm takes center stage in understanding how plants respond to abiotic stresses. *Plant Cell Rep.* 2013;32:945–57.
- Liu H, Guo SY, Lu MH, Zhang Y, Li JH, Wang W, Wang PT, Zhang JL, Hu ZB, Li LL, Si LY, Zhang J, Qi Q, Jiang XN, Botella JR, Wang H, Song CP. Biosynthesis of DHGA12 and its roles in Arabidopsis seedling establishment. *Nat Commun.* 2019;10:1768.
- Cheng BX, Peterson CM, Mitchell RJ. The role of sucrose, auxin and explant source on in vitro rooting of seedling explants of *Eucalyptus sideroxylon*. *Plant Sci.* 1992;87:207–14.
- De KGJ, Keppel M, Brugge JT, Meekes H. Timing of the phases in adventitious root formation in apple micro cutting. *J Exp Bot.* 1995;289:965–72.
- Wang L, Chu H, Li Z, Wang J, Li J, Qiao Y, Fu Y, Mou T, Chen C, Xu J. Origin and development of the root cap in rice. *Plant Physiol.* 2014;166:603–13.
- Sieberer T, Leyser O. Plant science-auxin transport, but in which direction? *Sci.* 2006;312:858–60.
- Yu J, Liu W, Liu J, Qin P, Xu L. Auxin control of root organogenesis from calus in tissue culture. *Front Plant Sci.* 2017;8:1385.
- Nag S, Saha K, Choudhuri MA. Role of auxin and polyamines in adventitious root formation in relation to changes in compounds involved in rooting. *J Plant Grow Reg.* 2001;20:182–94.
- Rout GR. Effect of auxins on adventitious root development from single node cuttings of *Camellia sinensis* (L.) Kuntze and associated biochemical changes. *Plant Grow Reg.* 2006;48:111–7.
- Cheng LB, Jiang RZ, Yang JJ, Xu XY, Zeng HT, Li SY. Transcriptome profiling reveals an IAA-regulated response to adventitious root formation in lotus seedling. *ZNC.* 2018;73c:229–40.
- Zeng YW, Verstraeten I, Trinh HK, Heugebaert T, Stevens CV, Garcia-Maquilon I, Rodriguez P, Vanneste S, Geelen D. *Arabidopsis* hypocotyl adventitious root formation is suppressed by ABA signaling. *Genes.* 2021;12:1141.
- Mu HZ, Jin XH, Ma XY, Zhao AQ, Gao YT, Lin L. Ortet age effect, anatomy and physiology of adventitious rooting in *tilia mandshurica* softwood cuttings. *Forests.* 2022;13:9.
- Steffens B, Wang JX, Sauter M. Interactions between ethylene, gibberellin and abscisic acid regulate emergence and growth rate of adventitious roots in deepwater rice. *Planta.* 2006;223:604–12.
- Han H, Sun XM, Xie YH, Feng J, Zhang SG. Anatomical and physiological effects of phytohormones on adventitious roots development in *larix kaempferi* L. *Olgensis.* *Silvae Genet.* 2013;62:3.
- Wang L, Hua DP, He JN, Duan Y, Chen ZZ, Hong XH, Gong ZZ. Auxin response factor2 (ARF2) and its regulated homeodomain gene HB33 mediate abscisic acid response in *Arabidopsis*. *Plos Genet.* 2011;7:e1002172.
- Wang JW, Wang LJ, Mao YB, Cai WJ, Xue HW, Chen XY. Control of root cap formation by microRNA-targeted auxin response factors in *Arabidopsis*. *Plant Cell.* 2005;17:2204–16.
- Waller F, Furuya M, Nick P. OsARF1, an auxin response factor from rice, is auxin-regulated and classifies as a primary auxin responsive gene. *Plant Mol Biol.* 2002;50:415–25.
- Qi YH, Wang SK, Shen CJ, Zhang SN, Chen Y, Xu YX, Liu Y, Wu YR, Jiang DA. OsARF12, a transcription activator on auxin response gene, regulates root elongation and affects iron accumulation in rice (*Oryza sativa* L.) [C]. *New Phytol.* 2011;193:1461–8.
- Feng ZH, Zhu J, Du XL, Cui XH. Effects of three auxin-inducible LBD members on lateral root formation in *Arabidopsis thaliana*. *Planta.* 2012;236:1227–37.
- Shin R, Burch AY, Huppert KA, Tiwari SB, Murphy AS, Guilfyle TJ, Schachtman DP. The *Arabidopsis* transcription factor MYB77 modulates auxin signal transduction. *Plant Cell.* 2007;19:2440–53.
- Sorin C, Bussell JD, Camus I, Ljung K, Kowalczyk M, Geiss G, Mckhann H, Garcia C, Vaucheret H, Sandberg G, Bellini C. Auxin and light control of adventitious rooting in *Arabidopsis* require *ARGONAUTE1*. *Plant Cell.* 2005;17:1343–59.
- Liu SA, Yang CX, Wu L, Cai H, Li HG, Xu M. The peu-miR160a-PeARF17.1/PeARF17.2 module participates in the adventitious root development of poplar. *Plant Bioech J.* 2020;18:457–69.

34. Cheng LB, Zhao MR, Hu ZB, Liu HY, Li SY. Comparative transcriptome analysis revealed the cooperative regulation of sucrose and IAA on adventitious root formation in lotus (*Nelumbo nucifera* Gaertn). *BMC Genomics*. 2020a;21:653.
35. Cheng LB, Han YY, Zhao MR, Li SY. Gene expression profiling reveals the effects of light on adventitious root formation in lotus seedlings (*Nelumbo nucifera* Gaertn). *BMC Genomics*. 2020b;21:707.
36. Clough SJ, Bent AF. Floral dip: a simplified method for *Agrobacterium*-mediated transformation of *Arabidopsis thaliana*. *Plant J*. 1998;16:735–43.
37. Ross ARS, Stephen AJ, Adrian CJ, Feurtado JA, Kermod AR, Nelson K, Zhou R, Abrams SR. Determination of endogenous and supplied deuterated abscisic acid in plant tissues by high-performance liquid chromatography-electrospray ionization tandem mass spectrometry with multiple reaction monitoring. *Anal Biochem*. 2004;329:324–33.
38. Kojima M, Kamada-Nobusada T, Komatsu H, Takei K, Kuroha T, Mizutani M, Ashikari M, Ueguchi-Tanaka M, Matsuoka M, Suzuki K. Highly sensitive and high-throughput analysis of plant hormones using MS-probe modification and liquid chromatography-tandem Mass Spectrometry: an application for hormone profiling in *Oryza sativa*. *Plant Cell Physiol*. 2009;50:1201–14.
39. Nhujak T, Srisa-Art M, Kalsapakorn K, Tolieng V, Petsom A, Petsom A. Determination of gibberellic acid in fermentation broth and commercial products by micellar electrokinetic chromatography. *J Agric Food Chem*. 2005;53:1884–9.
40. Vanneste S, Friml J. Auxin: a trigger for change in plant development. *Cell*. 2009;136:1005–16.
41. Wei HB, Cui BM, Ren YL, Li JH, Liao WB, Xu NFei, Peng M. Research progresses on auxin response factors. *J Integr Plant Biol*. 2006;48:622–7.
42. Jin LF, Yarra R, Zhou LX, Cao HX. The auxin response factor (ARF) gene family in oil palm (*Elaeis guineensis* Jacq.): genome-wide identification and their expression profiling under abiotic stresses. *Protoplasma*. 2022;259:47–60.
43. Hagen G, Guilfoyle T. Auxin-responsive gene expression: genes, promoters and regulatory factors. *Plant Mol Biol*. 2002;49:373–85.
44. Tiwari SB, Hagen G, Guilfoyle TJ. The roles of auxin response factor domains in auxin-responsive transcription. *Plant Cell*. 2003;5:533–43.
45. Liscum E, Reed JW. Genetics of Aux/IAA and ARF action in plant growth and development. *Plant Mol Biol*. 2002;49:387–400.
46. William CJ. Auxin Response Factors. *J Plant Cell Environ*. 2016;39: 1014–28. Res. 2002;14:131–43.
47. Wang YJ, Deng DX, Shi YT, Miao N, Bian YL, Yi ZT. Diversification, phylogeny and evolution of auxin response factor (ARF) family: insights gained from analyzing maize ARF genes. *Mol Biol Rep*. 2012;39:2401–15.
48. Wei SY, Chen YN, Hou J, Yang YH, Yin TM. Aux/IAA and ARF gene families in *Salix suchowensis*: identification, evolution, and dynamic transcriptome profiling during the plant growth process. *Front Plant Sci*. 2021;12:666310.
49. Gil CS, Jung HY, Lee C, Eom SH. Blue light and NAA treatment significantly improve rooting on single leaf-bud cutting of *Chrysanthemum* via upregulated rooting-related genes. *Sci Hortic*. 2020;274:109650.
50. Della Rovere F, Fattorini L, D'Angeli S, Velocchia A, Falasca G, Altamura MM. Auxin and cytokinin control formation of the quiescent centre in the adventitious root apex of *Arabidopsis*. *Ann Bot*. 2013;112:1395–407.
51. Fukaki H, Tasaka M. Hormone interactions during lateral root formation. *Plant Mol Biol*. 2009;69:437–49.
52. Gutierrez L, Bussell JD, Păcurar DI, Schwambach J, Păcurar M, Bellini C. Phenotypic plasticity of adventitious rooting in *Arabidopsis* is controlled by complex regulation of auxin response factor transcripts and MicroRNA abundance. *Plant Cell*. 2009;21:3119–32.
53. Staswick PE, Tiriyaki I, Rowe M. Jasmonate response locus *JAR1* and several related *Arabidopsis* genes encode enzymes of the firefly luciferase superfamily that show activity on jasmonic, salicylic, and indole-3-acetic acids in an assay for adenylation. *Plant Cell*. 2002;14:1405–15.
54. Kuhn N, Serrano A, Abello C, Arce A, Espinoza C, Gouthu S, Deluc L, Arce-Johnson P. Regulation of polar auxin transport in grapevine fruitlets (*Vitis vinifera* L.) and the proposed role of auxin homeostasis during fruit abscission. *BMC Plant Biol*. 2016;16:234.
55. Reingardt D, Pesce ER, Stieger P, Mandel T, Baltensperger K, Bennett M, Traas J, Friml J, Kuhlemeier C. Regulation of phyllotaxis by polar auxin transport. *Nat*. 2003;426:255–60.
56. Schatlowski N, Creasey K, Goodrich J, Schubert D. Keeping plants in shape: polycomb-group genes and histone methylation. *Semin Cell Dev Biol*. 2008;19:547–53.
57. Sun FF, Zhang WS, Hu HZ, Li B, Wang YN, Zhao YK, Li KX, Liu MY, Li X. Salt modulates gravity signaling pathway to regulate growth direction of primary roots in *Arabidopsis*. *Plant Physiol*. 2008;146:178–88.
58. Nishimura T, Nakano H, Hayashi KI, Niwa C, Koshiba T. Differential downward stream of auxin synthesized at the tip has a key role in gravitropic curvature via TIR1/AFBs-mediated auxin signaling pathways. *Plant Cell Physiol*. 2009;50:1874–85.
59. Naqvi SM, Gordon SA. Auxin transport in *Zea mays* L. Coleoptiles I. Influence of gravity on the transport of Indoleacetic Acid-2-14C1. *Plant Physiol*. 1966;41:1113–8.
60. Marchant A, Bhalerao R, Casimiro I, Eklöf J, Casero PJ, Bennett M, Sandberg G. *AUX1* promotes lateral root formation by facilitating indole-3-acetic acid distribution between sink and source tissues in the *Arabidopsis* seedling. *Plant Cell*. 2002;14:589–97.
61. Carraro N, Tisdale-Orr TE, Clouse RM, Knoller AS, Spicer R. Diversification and expression of the PIN, AUX/LAX, and ABCB families of putative auxin transporters in *Populus*. *Front Plant Sci*. 2012;3:17.
62. Li CX, Hou XM, Mou KP, Liu HW, Zhao ZX, Liao WB. The involvement of abscisic acid in glucose promoted adventitious root development in cucumber. *Sci Hortic*. 2002a;295:110816.
63. Li CX, Zhang ML, Qi NN, Liu HW, Zhao ZX, Huang PP, Liao WB. Abscisic acid induces adventitious rooting in cucumber (*Cucumis sativus* L.) by enhancing sugar synthesis. *Plants-Basel*. 2002b;11:2354.
64. Tartoura KAH. Effect of abscisic acid on endogenous IAA, auxin protector levels and peroxidase activity during adventitious root initiation in *Vigna radiata* cuttings. *Acta Physiol Plant*. 2001;23:149–56.
65. Wei H, Liu QZ, Zong XJ, Wang JW, Zhang D, Chen X, Xu L. Effects of IBA on adventitious root development and the associated metabolic changes during softwood cutting rooting of sweet cherry rootstocks Gisela 6. *Acta Hort*. 2017;1161:67.
66. Lagrimini LM, Joly RJ, Dunlap JR, Liu TTY. The consequence of peroxidase overexpression in transgenic plants on root growth and development. *Plant Mol Biol*. 1997;33:887–95.
67. McDonald MS, Wynne J. Adventitious root formation in woody tissue: Peroxidase—a predictive marker of root induction in *Betula pendula*. *Vitro Cell Dep-PL*. 2003;39:234–5.
68. Meng XY, Wang Z, He SL, Shi LY, Song YL, Lou XY, He D. Endogenous hormone levels and activities of IAA-modifying enzymes during adventitious rooting of tree peony cuttings and grafted scions. *Hort Environ Biotech*. 2019;60:187–97.
69. Ahkami AH, Melzer M, Ghaffari MR, Pollmann S, Javid MG, Shahinnia F, Hajirzaei MR, Druge U. Distribution of indole-3-acetic acid in *Petunia* hybrid shoot tip cuttings and relationship between auxin transport, carbohydrate metabolism and adventitious root formation. *Planta*. 2013;238:499–517.
70. Chen D, Wang WA, Wu YQ, Xie H, Zhao LF, Zeng Q, Zhan YH. Expression and distribution of the auxin response factors in sorghum bicolor during development and temperature stress. *Int J Mol Sci*. 2019;20:4816.
71. Verma S, Negi NP, Pareek S, Mudgal G, Kumar D. Auxin response factors in plant adaptation to drought and salinity stress. *Physiol Plant*. 2022;174:e13714.
72. Ren HB, Gao ZH, Chen L, Wei KF, Liu J, Fan YJ, Davies WJ, Jia WS, Zhang JH. Dynamic analysis of ABA accumulation in relation to the rate of ABA catabolism in maize tissues under water deficit. *J Exp Bot*. 2007;58:211–9.
73. Nakashima K, Yamaguchi-Shinozaki K. ABA signaling in stress-response and seed development. *Plant Cell Rep*. 2013;32:959–70.
74. Seki M, Narusaka M, Ishida J, Nanjo T, Fujita M, Oono Y, Kamiya A, Nakajima M, Enju A, Sakurai T, Satou M, Akiyama K, Taji T, Yamaguchi-Shinozaki K, Carninci P, Kawai J, Hayashizaki Y, Shinozaki K. Monitoring the expression profiles of 7000 *Arabidopsis* genes under drought, cold and high-salinity stresses using a full-length cDNA microarray. *Plant J*. 2002;31:279–92.
75. Ha M, Li WH, Chen ZJ. External factors accelerate expression divergence between duplicate genes. *Trends Genet*. 2007;23:162–6.

Publisher's Note

Springer Nature remains neutral with regard to jurisdictional claims in published maps and institutional affiliations.